Agricultural and Forest Meteorology 362 (2025) 110366

Contents lists available at ScienceDirect

Agricultural and Forest Meteorology

journal homepage: www.elsevier.com/locate/agrformet

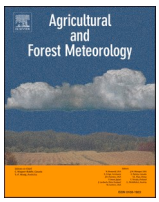

Changes in leaf and root carbon allocation of global vegetation simulated by the optimally integrated ecosystem models

Zeyu Duanmu [a,b], Zaichun Zhu [a,b,*], Weiqing Zhao [a,b], Anping Chen [c], Zhaoqi Wang [d], Sen Cao [a,b], Dajing Li [a,b], Yuhang Luo [a,b], Ranga B. Myneni [e]

[a] School of Urban Planning and Design, Peking University, Shenzhen 510855, China
[b] Key Laboratory of Earth Surface System and Human-Earth Relations, Ministry of Natural Resources of China, Shenzhen Graduate School, Peking University, Shenzhen 510855, China
[c] Department of Biology and Graduate Degree Program in Ecology, Colorado State University, Fort Collin, CO 80523, USA
[d] State Key Laboratory of Plateau Ecology and Agriculture, Qinghai University, Xining 810016, China
[e] Department of Earth and Environment, Boston University, Boston, MA 02215, USA

ARTICLE INFO

Keywords:
Carbon allocation
Root and leaf
Global vegetation
Climate change
Ecosystem models

ABSTRACT

Carbon allocation in vegetation, particularly to leaves and roots responsible for resource assimilation, plays a crucial role in regulating the global carbon cycle and is highly sensitive to environmental changes. However, due to the limited observational data, the response of carbon allocation—particularly between resource-acquiring organs—to rapid global environmental changes remains unclear for global vegetation. State-of-the-art ecosystem models provide valuable insights into the spatiotemporal patterns of carbon allocation across global vegetation. In this study, we developed a weighted model average (WMA) by optimally integrating ecosystem models based on their performance in simulating the spatiotemporal changes in root and leaf carbon. The WMA well captured the satellite-observed leaf carbon trend and the spatial variations in root carbon along climate gradients ($R^2 = 0.82$). The WMA suggested global vegetation has increasingly allocated more carbon to roots than leaves (the trend of allometric scaling relations between leaf and root: 0.0014 ± 0.0013 g g^{-1} yr^{-1}, $p < 0.05$) during 1982–2018. Elevated atmospheric CO_2 concentration was the dominant driver of changes in root/leaf carbon allocation globally (0.0010 ± 0.0005 g g^{-1} yr^{-1}, $p < 0.05$), particularly in tropical regions. Climate change influenced carbon allocation in vegetation differently across regions, contributing to increased root carbon allocation in the Northern Hemisphere and enhanced leaf carbon allocation in tropical areas. Land use change led to more carbon being allocated to leaves than roots (-0.0003 ± 0.0006 g g^{-1} yr^{-1}, $p < 0.05$). Overall, we tentatively quantified the changes in the carbon allocation to the leaf and root across global terrestrial vegetation under the dramatic environmental change based on WMA, which helps further understanding of the changes in the functioning of the terrestrial ecosystem and reasonable projection of changes in the future global carbon cycle.

1. Introduction

Vegetation carbon allocation is vital for the development and functioning of the terrestrial ecosystems. Within the vegetation components, organs perform a range of functions (Mokany et al., 2006; Poorter et al., 2012) and influence the physiological functions. Specifically, leaf carbon could partially account for terrestrial photosynthetic uptake (Kala et al., 2014; Zhao and Zhu, 2022; Zhu et al., 2016), stem carbon constitutes the hydraulic pathway (Poorter et al., 2012), and the root carbon as well as its coordination with soil microbial are associated with soil organic carbon through soil respiration (Borden et al., 2021; Dijkstra et al., 2021; Tian et al., 2010). Vegetation sustains optimal growth through carbon allocation to adapt to external stress. For example, it can increase belowground carbon allocation to maintain stable productivity under climate warming (Liu et al., 2018) or to sustain resilience after drought events (Hagedorn et al., 2016). From the perspective of carbon storage, carbon allocation influences the subsequent fate of carbon, as the vegetation tissues have different turnover rates, such as the long-lived organs (stem and coarse roots) and short-lived organs (leaf and fine roots). As a consequence, carbon residence time further

* Corresponding author.
E-mail address: zhu.zaichun@pku.edu.cn (Z. Zhu).

https://doi.org/10.1016/j.agrformet.2024.110366
Received 16 May 2024; Received in revised form 4 December 2024; Accepted 10 December 2024
Available online 19 December 2024

Table 1
TRENDY models used in this study.

Model	Carbon allocation strategy	Reference
CABLE-POP	Allometric, fixed allocation based on phenology and functional type.	(Wang et al., 2009)
CLASS-CTEM	Optimal, according to water availability and light, allocation is a constant based on leaf onset or limiting conditions.	(Asaadi et al., 2018; Krinner et al., 2005)
CLM5.0	Allometric, allocation is a constant for woody plants based on functional types.	(Lawrence et al., 2019)
ISAM	Optimal, according to water, light, and nitrogen availability, allocation is a constant based on leaf onset or limiting conditions.	(Arora and Boer, 2005; El-Masri et al., 2013)
LPX-Bern	Optimal–allometric, leaf area-to-sapwood area ratio is fixed, leaf and root biomass are controlled by the functional type-dependent leaf-to-root mass ratio, and N and water availability.	(Sitch et al., 2003)
ORCHIDEE	Optimal, determined by water, light, and nitrogen availability	(Krinner et al., 2005)
ORCHIDEE-CNP	Optimal, determined by water, light, and nitrogen availability	(Krinner et al., 2005; Sun et al., 2021)

determines the terrestrial carbon budget (Luo et al., 2003). Recent studies emphasized the importance of carbon allocation in accurately estimating terrestrial carbon stocks and fluxes (Bloom et al., 2016; Friedlingstein et al., 1999; Friend et al., 2014; Ruehr et al., 2023; Vicca et al., 2012).

Vegetation carbon allocation reflects the priority of resource acquisition (Bloom et al., 1985; Thornley, 1972), and is sensitive to environmental changes (Dolezal et al., 2021; Meng et al., 2023; Song et al., 2019; Zhou et al., 2020). Since the Industrial Revolution (IPCC, 2021), the availability of resources for vegetation has been altered by global environmental changes, such as elevated atmospheric CO_2 concentration, climate change, nitrogen deposition, and land use change. Leaves and roots, being resource-acquiring organs responsible for photosynthesis and the uptake of soil-based resources, respectively, are more sensitive to changes in resource availability compared to stems, which primarily provide structural support and biomass storage (Mokany et al., 2006; Poorter et al., 2012). The changes in resource availability and the subsequent responses of leaves and roots affect the structure and functioning of vegetation (Pearcy et al., 2005; Poorter et al., 2012).

The lack of spatiotemporally consistent datasets on vegetation carbon pools at the global scale (Bloom et al., 2016; Fatichi et al., 2019), especially the global root carbon measurements (Song et al., 2017), prevents further study about the changes and mechanisms of carbon allocation. Various methods, such as meta-analysis (Eziz et al., 2017; Yue et al., 2021; Zhou et al., 2020), formula derivation (Palmroth et al., 2006), and manipulation experiments (Liu et al., 2018) have been used to study carbon allocation among different tissues. Existing studies on carbon allocation strategy are widely focused on plant scale (Aarssen and Taylor, 1992; Shipley and Meziane, 2002) due to the data availability (Mahmud et al., 2018). There is a long-running debate on whether carbon allocation strategies are fixed or varied along environmental gradients (McCarthy and Enquist, 2007).

Two main carbon allocation theories are optimal partitioning theory (Bloom et al., 1985; Thornley, 1972) and allometric partitioning theory (Müller et al., 2000). The premise of optimal partitioning theory is that under conditions of resource limitation (e.g., of water, nutrients, or light), plants will allocate more biomass to the organs most stressed by the lack of the limiting resource (Bloom et al., 1985). The allometric biomass partitioning theory is based on allometric theory, which posits that the allometric relationships between different tissues remain stable throughout the life cycle (Müller et al., 2000). Currently, all carbon allocation strategies integrated into ecosystem models follow fundamentally empirical descriptions (Franklin et al., 2012) with either of the above two theories or their combination (see Table 1).

Considering the uncertainties and large discrepancies that existed in the ensemble of state-of-the-art models (Eyring et al., 2019; Knutti et al., 2017), the conventional method is to calculate the multi-model ensemble mean (MMEM). This approach treats each model equally and is able to eliminate uncertainties in model intercomparison (Knutti, 2010; Knutti et al., 2017; Zhu et al., 2016). However, MMEM fails to take the models' performance into account (Flato et al., 2013) and neglects the interdependence among models (Flato et al., 2013; Knutti et al., 2017). As previously mentioned, ecosystem models share formulations on the basis of two theories to describe carbon allocation (Table 1). Consequently, these models are not truly random or independent in the carbon allocation module (Fisher et al., 2014). Alternatively, the "reliability ensemble average" approach employs a weighting scheme based on model performance (Giorgi and Mearns, 2002). As better-performed models have larger weights, the weighting average scheme can boost the confidence of projections over MMEM and individual models (Exbrayat et al., 2018; Eyring et al., 2019; Knutti et al., 2017), and has been used to investigate the historical changes and future projection of vegetation growth under global change (Zhao et al., 2020; Zhu et al., 2017).

This study aims to investigate the changes and driving mechanisms of carbon allocation between leaf and root of global vegetation from 1982 to 2018. Firstly, we evaluated the spatial and temporal changes in leaf carbon and root carbon of seven ecosystem models. Then, we optimally integrated seven state-of-the-art ecosystem models through a weighted average scheme based on the model performance. Further, we investigated the carbon allocation between leaf and root through the weighted model average. Finally, we disentangled the contributions of increasing CO_2 concentration, climate change, land cover and land use change on carbon allocation between leaf and root.

2. Data and methods

2.1. Ecosystem models

We obtained ecosystem model outputs from the "Trends and drivers of the regional scale sources and sinks of carbon dioxide" project phase 8 (TRENDY v8) from 1982 to 2018. Seven ecosystem models including CABLE-POP, CLASS-CTEM, CLM5.0, ISAM, LPX-Bern, ORCHIDEE, and ORCHIDEE-CNP were selected and two target variables, i.e., root carbon density and leaf carbon density, were extracted. Three types of allocation strategies were used in the models (Table 1). In optimal models, carbon was allocated to the resource-limited organs. In allometric models, a fixed fraction of NPP was imposed on each organ. In optimal-allometric models, the allocation fractions of leaf and root were determined with external stress, combined with an extra constraint among leaf area and sapwood area. The root carbon density and leaf carbon density in the models were represented by annual maximum values. Root carbon has accounted for both fine and coarse roots.

A series of factorial simulations were conducted by TRENDY v8 including simulation S0 to S3. In simulation S0, models were run without forcing change, aside from recycling climate means and variability from the 1920s. In simulation S1, models were forced with historical CO_2 concentrations and recycling of climate means and variability from the 1920s. Both atmospheric CO_2 concentrations and climate were variable in simulation S2. In simulation S3, models were forced with CO_2 concentrations, climate change, and changes in land use and land cover. The multi-model ensemble estimates for root and leaf carbon were derived from S3, and we regarded S3 as the situation closest to the historical record. The effects of elevated CO_2 concentrations, climate change, and land use and land cover changes on carbon allocation between root and leaf were derived from S1 – (minus) S0, S2 – S1, and S3 – S2, respectively.

2.2. Leaf and root carbon data

Leaf carbon was calculated based on the relationship between the

leaf area index (LAI) and specific leaf area (SLA) (1). We used the average of three satellite-observed LAI products of global vegetation for the period 1982–2016, including the Global Inventory Modelling and Mapping Studies third-generation LAI product (GIMMS LAI3g) (Zhu et al., 2013), the Global Mapping LAI product (GLOBMAP LAI) (Liu et al., 2012), and the Global Land Surface Satellites LAI product (GLASS LAI) (Xiao et al., 2014). The global SLA dataset was created by extrapolating site-based observations to the global scale using a Bayesian spatial model (Butler et al., 2017). We compared model-derived estimates of leaf carbon to observed leaf carbon data.

$$\text{Leaf carbon} = \text{LAI}/\text{SLA} \tag{1}$$

Where LAI refers to the maximum annual values ($m^2\ m^{-2}$), and SLA is in $m^2\ g^{-1}$. Root carbon was calculated from the root mass fraction (RMF) and aboveground biomass (AGB) (2). RMF was estimated using Random Forest models, based on the relationship between site-level RMF measurements and multiple environmental layers (Ma et al., 2021). AGB data was provided by the Intergovernmental Panel on Climate Change (IPCC) Tier 1 (Ruesch and Gibbs, 2008). Then the root carbon was calculated as half of the root biomass based on an empirical relationship (Buffam et al., 2011).

$$\text{Root biomass} = \text{AGB} \times \frac{\text{RMF}}{1-\text{RMF}} \tag{2}$$

2.3. Meteorological data sets

To analyze the spatial pattern of root carbon and root/leaf carbon allocation along the climate zones, the meteorological datasets were acquired from Climate Research Unit (CRU) TS4.03 (https://crudata.uea.ac.uk/cru/data/hrg/cru_ts_4.03/). CRU TS4.03 provided long-term global coverage meteorology data variables with 0.5° × 0.5° spatial resolution (Harris et al., 2020). They were used in the historical forcing data in TRENDY v8 from 1901 to 2018. Given the climate condition was fixed at 'pre-industrial' under simulations S0 and S1 with the recycling climate mean and variability from 1901 to 1920, we used the mean temperature, the mean precipitation, and actual vapor pressure in the growing season in the analysis of CO_2 contribution to allocation. The growing season was defined as the collection of months that were above 0 °C. The vapor pressure deficit was derived from the difference between saturation vapor pressure and actual vapor pressure.

2.4. Metric of carbon allocation between leaf and root

To better investigate the response of allocation under global change, it is vital to control for the potential influencing factors such as site age and plant size (Poorter and Nagel, 2000). The scaling relationships of log-transformed biomass in different tissues (leaf, stem, and root) are robust among different orders of magnitude in diverse communities (Enquist and Niklas, 2002), and have been shown to be an index independent of plant ontogeny compared with ratio (such as leaf: root) (McCarthy and Enquist, 2007). Thus, it can be a valid proxy of allocation between leaf and root carbon at the global scale. In this article, the relationship of root and leaf carbon (in grams) derived from the models was log 10-transformed. The regression of log 10-transformed root and leaf carbon was considered to represent the carbon allocation results between leaf and root (Enquist and Niklas, 2002) (3).

$$log_{10}^{root\ carbon} = \alpha \times log_{10}^{leaf\ carbon} + \beta \tag{3}$$

The scaling exponent α represents the quantitative carbon allocation relationship between leaf and root carbon (hereafter, root/leaf carbon allocation). A positive value indicates a tendency whereby more carbon is allocated to the roots than to leaves and vice versa. β is an allometric constant that may vary among species. We excluded root/leaf carbon allocation greater than 3 g g^{-1} and smaller than −3 g g^{-1} to minimize the outliers. Trends in root/leaf carbon allocation were calculated in 10-year moving windows, the schematic diagram of root/leaf carbon allocation is displayed in Fig. S1.

2.5. Optimally integrated models

We employed the optimally integrated models through a weighted model average (WMA) based on the historical performance of leaf and root carbon simulation. In this study, the WMA root/leaf carbon allocation was calculated through the weighted average of root/leaf carbon allocation by each model, that is,

$$\widetilde{\alpha} = \frac{\sum_{i=1}^{N} w_i \times \alpha_i}{\sum_{i=1}^{N} w_i} \tag{4}$$

Where α_i is the root/leaf carbon allocation (and the corresponding contribution of elevated atmospheric CO_2, climate change, and land cover change, respectively) simulated by model i, $\widetilde{\alpha}$ is the root/leaf carbon allocation (and the above three effects) estimated by the WMA, N is the total number of ecosystem models, and w_i is the weight of model i (5):

$$w_i = \left[\left(R_{\text{leaf spatial, i}}\right)^a \times \left(R_{\text{root spatial, i}}\right)^b \times \left(R_{\text{leaf temporal, i}}\right)^c\right]^{(1/a\times b\times c)} \tag{5}$$

Where w_i is the weight factor that reflects the performance of leaf carbon and root carbon from model i. $r_{\text{leaf spatial, i}}$, $r_{\text{root spatial,i}}$, and $r_{\text{leaf temporal, i}}$ were calculated. $r_{\text{leaf spatial, i}}$ measures the spatial correlation coefficient of leaf carbon according to seven vegetation types (Fig. S2). $r_{\text{root spatial,i}}$ was calculated as the correlation coefficient between observation and model outputs for the average root biomass in all the growing season climate intervals. The interval of growing season climate space is 2 °C for temperature and 200 mm $month^{-1}$ for precipitation. $r_{\text{leaf temporal, i}}$ reflects the temporal correlation coefficient of leaf carbon averaged at a 3 × 3 grid window. We further normalized $r_{\text{leaf spatial, i}}$, $r_{\text{root spatial,i}}$, and $r_{\text{leaf temporal, i}}$ to 0–1 and derived $R_{\text{leaf spatial, i}}$, $R_{\text{root spatial, i}}$ and $R_{\text{leaf temporal, i}}$ in Eq. (5). a, b, and c are the power of each weighting factor. We tested the robustness of the simulated results with a set of combinations of three powers (a, b and c) (Fig. S3, S4) and selected the best one ($a = 1$, $b = 1$, $c = 2$).

2.6. Evaluation metrics for ecosystem models

We evaluated the performance of each ecosystem model in spatial and temporal aspects, including the spatial correlation of root carbon and leaf carbon, the temporal correlation of leaf carbon, the bias of leaf carbon time series, and the trend bias of leaf carbon. The spatial correlation of leaf carbon ($r_{\text{leaf spatial, global}}$) and root carbon ($r_{\text{root spatial, global}}$) and the temporal correlation of global leaf carbon time series ($r_{\text{leaf temporal, global}}$) was calculated for all the vegetated grids. The bias of the leaf carbon and its trend were quantified as the absolute difference between the model and observation.

$$\text{bias} = \sum_{i=1}^{n} \left|\gamma_i^{\text{sim}} - \gamma_i^{\text{obs}}\right| \tag{6}$$

Where γ_i^{sim} is the predicted value of leaf carbon time series in the i^{th} year, γ_i^{obs} represents the i^{th} leaf carbon time series from observation, and n is from 1982 to 2016. We summed the absolute model error during the study period using Eq. (6), and then normalized it as the bias index (7), by dividing the maximum bias of all ecosystem models.

$$\text{bias index} = 1 - \frac{\text{bias}_m}{\max(\text{bias}_m)} \tag{7}$$

Where the bias_m is leaf carbon bias for model m. The bias index ranges from 0 to 1, where 1 corresponds to the best-performing model and 0 to the worst. The trend bias of leaf carbon was calculated as the absolute error between the model and observation (8). It was then normalized as trend bias index according to (7) for consistency.

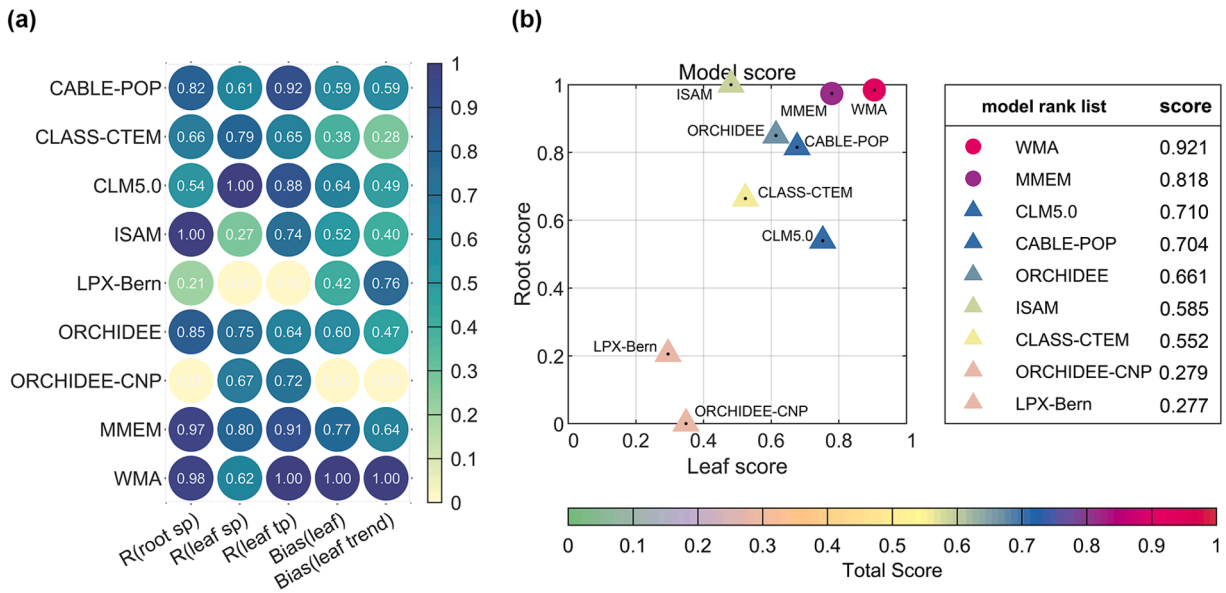

Fig. 1. Evaluation of leaf carbon and root carbon of seven ecosystem models and their ensemble means. (a) The model performance under five evaluation indices. (b) The model performance for leaf, root, and the overall integration. A score of zero represents the worst performance among all the models, and a score of one indicates the best. All the ecosystem models were evaluated under 'S3' scenarios.

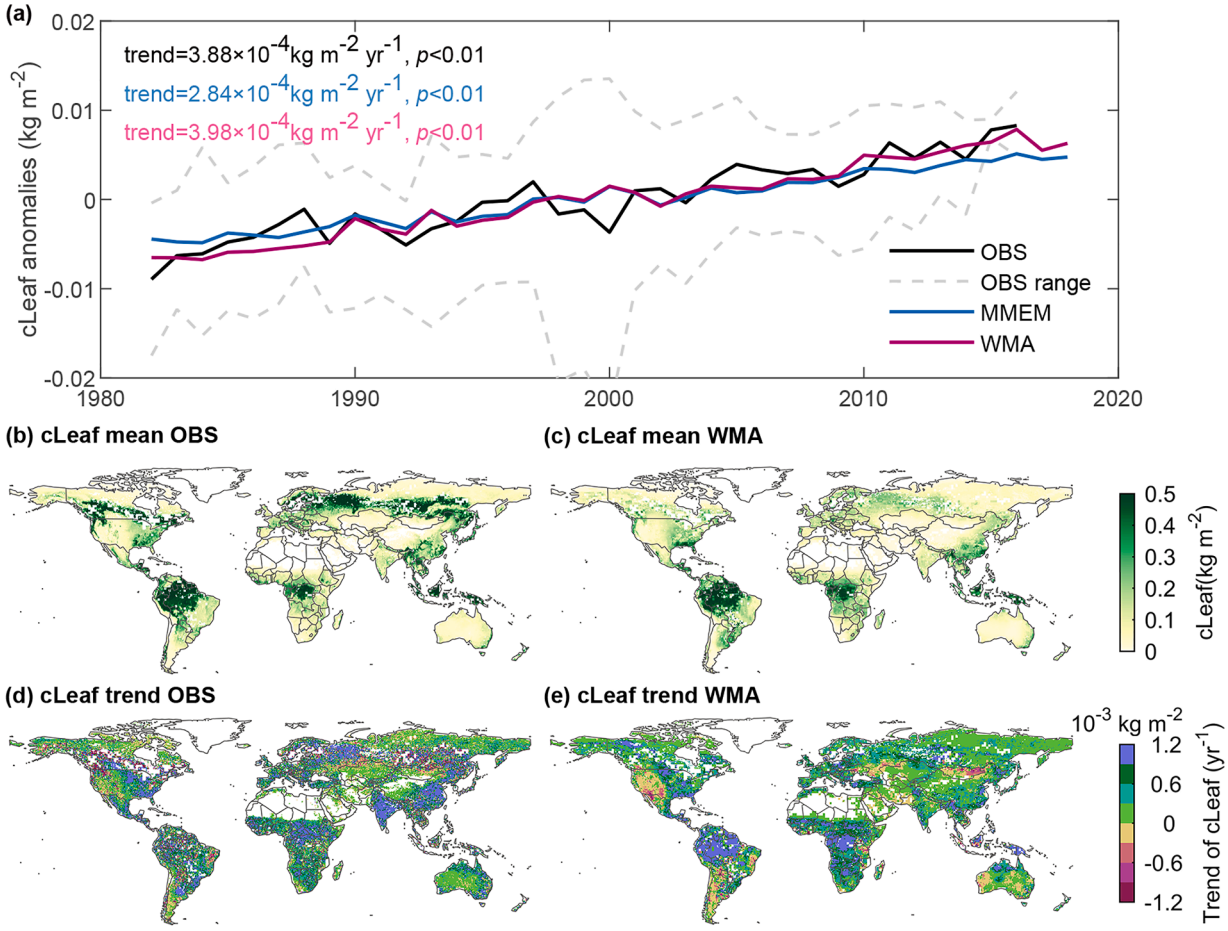

Fig. 2. Temporal changes of global cLeaf from 1982 to 2016. (a) Changes of global cLeaf from 1982 to 2016 for observation (black line) and for simulation integrated with MMEM in the blue line and WMA in the pink line between 1982 and 2018. The dashed gray lines represent the range of 3 observed cLeaf references. (b-e) The spatial pattern of the annual mean of cLeaf and the trend of cLeaf for observation and WMA. All the ecosystem models are evaluated under 'S3' scenarios.

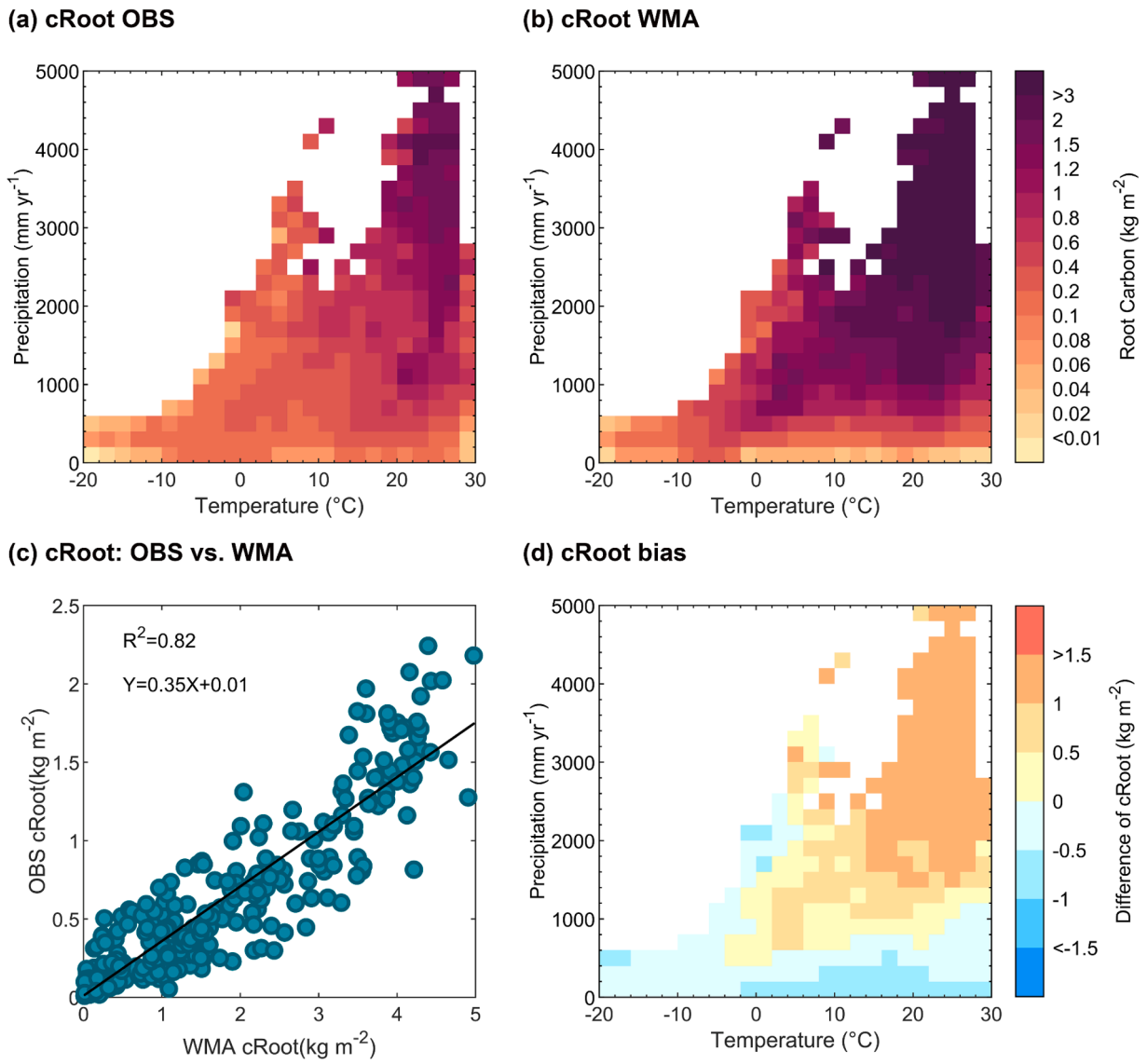

Fig. 3. Root carbon distribution along gradients of the growing season mean temperature and total precipitation in (a) the global root carbon dataset (OBS), and (b) WMA ('S3' scenarios). (c) The relationship of root carbon estimated between WMA and OBS, and (d) the difference between WMA and OBS in environmental space.

$$\text{trend bias} = \left|t^{sim} - t^{obs}\right| \tag{8}$$

Finally, we normalized all the above five indices as $R_{root\ spatial,\ global}$, $R_{leaf\ spatial,\ global}$, $R_{leaf\ temporal,\ global}$, Bias index, and Trend bias index to 0–1 before combining them into root dimension, leaf dimension and a single score (9) to evaluate the performance of each model.

$$score = \frac{R_{root\ spatial,\ global}}{\text{number of root index}} + \frac{R_{leaf\ spatial,global} + R_{leaf\ temporal,global} + \text{Bias index} + \text{Trend bias index}}{\text{number of leaf indexes}} \tag{9}$$

Where the number of root index is 1, and the number of leaf indices is 4. Scores range from 0 to 1. Scores close to 1 indicate that the model predictions are close to observed values.

3. Results

3.1. Evaluation of ecosystem models

We evaluated the ecosystem models in representing the spatiotemporal pattern of leaf carbon and root carbon (Fig. 1a). The performance of the model simulation was quantified in five aspects: the spatial correlation coefficient of leaf carbon and root carbon ($R_{leaf\ sp}$ and $R_{root\ sp}$), the bias and the trend bias of leaf carbon time series ($Bias_{leaf}$ and $Bias_{leaf\ trend}$), and the temporal correlation coefficient of leaf carbon time series ($R_{leaf\ tp}$). The $R_{root\ sp}$ ranged from 0.390 (ORCHIDEE-CNP) to 0.790 (ISAM), the $R_{leaf\ sp}$ ranged from 0.380 (LPX-Bern) to 0.786 (CLM5.0), and the $R_{leaf\ tp}$ varied from 0.803 (LPX-Bern) to 0.899 (CABLE-POP). LPX-Bern and CLM5.0 represented the closest to observation in $Bias_{leaf\ trend}$ (8.25×10^{-5} kg m^{-2} year^{-1}) and $Bias_{leaf}$ (0.068 kg m^{-2}), respectively. All models performed well for at least two indices. CABLE-POP, ORCHIDEE, and CLM5.0 provided relatively good estimates of all indices, whereas ORCHIDEE-CNP produced the worst estimates of interannual variations and trends in leaf carbon and spatial patterns in root carbon, respectively. Multi-model ensemble enhanced the performance of leaf carbon and root carbon. In particular, the $R_{leaf\ tp}$, $Bias_{leaf\ trend}$, and $Bias_{leaf}$ based on WMA performed the best among all the ecosystem models.

We then integrated the five indices for the leaf and root dimensions, before combining the scores into a final score (Fig. 1b). In general, all models performed well except ORCHIDEE-CNP. The overall model score of WMA showed the highest performance, with a final score of 0.921,

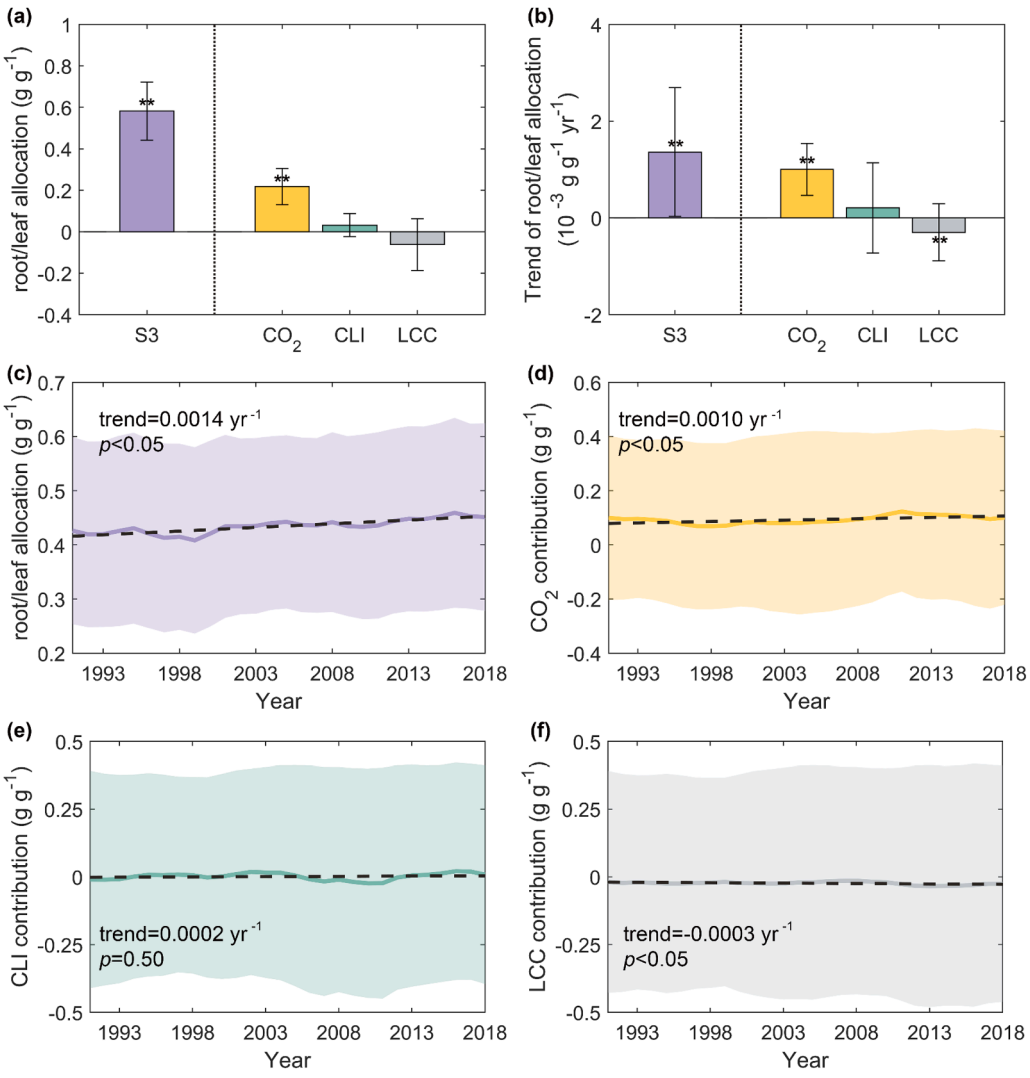

Fig. 4. The global vegetation root/leaf carbon allocation and its drivers from the weighted model average (WMA) between 1982 and 2018. (a) The root/leaf carbon allocation and its drivers during the period from 1982 to 2018. (b) Trend in root/leaf carbon allocation and its drivers in the same period. The error bar indicates the standard deviation from 7 ecosystem models, and the asterisks illustrate statistically significant contributions ($p < 0.05$). Time series in (c) represent the root/leaf carbon allocation with contributions from (d) CO_2, (e) climate change (CLI), and (f) land cover and land use change (LCC).

followed by MMEM with a final score of 0.818. The integrated model performance of WMA was significantly better than MMEM with 12.6 % improvements ($p < 0.01$), through the *t*-test of seven parameter combinations (Fig. S3). CLM5.0 attained the highest final score (0.710) among individual models. CABLE-POP (0.704) and ORCHIDEE (0.661) also performed well relative to ISAM, CLASS-CTEM, ORCHIDEE-CNP and LPX-Bern. ORCHIDEE-CNP and LPX-Bern failed to capture the spatial distribution of global root carbon and the temporal changes in leaf carbon. The models had different strengths and weaknesses. For example, CLM5.0 performed relatively well for leaves but not roots, whereas ISAM was among the best models for roots but performed poorly for leaves.

3.2. *Spatiotemporal changes in global root and leaf carbon based on WMA*

We used leaf carbon (cLeaf) reference to evaluate the performance of WMA (Fig. 2a) and individual ecosystem models (Fig. S5). Both observed and modeled cLeaf displayed an increasing trend ($cLeaf_{OBS}$ trend=3.88×10^{-4} kg m^{-2} yr^{-1}, $cLeaf_{MMEM}$ trend=2.84×10^{-4} kg m^{-2} yr^{-1}, and $cLeaf_{WMA}$ trend=3.98×10^{-4} kg m^{-2} yr^{-1}). Compared to the cLeaf trend of observed data, however, the spread of WMA (0.10×10^{-4} kg m^{-2} yr^{-1}) was smaller than that of MMEM (1.04×10^{-4} kg m^{-2} yr^{-1}). WMA corrected the underestimation of the cLeaf trend in MMEM. WMA provided a trend of cLeaf that was closer to the observation and had a higher temporal correlation coefficient ($r = 0.924$) than that of MMEM (0.917).

Fig. 2b-c illustrate the spatial pattern of the cLeaf annual mean and trend during the period from 1982 to 2016. The largest annual mean cLeaf values were observed in the needleleaf forests in northern high latitudes and the broadleaf forests in tropical regions, such as the Amazon basin, central Africa, Indonesia, and Malaysia, with cLeaf values close to 0.50 kg m^{-2}. Conversely, the small cLeaf values were primarily distributed in global drylands, notably in shrublands and grasslands with cLeaf values < 0.10 kg m^{-2} (Fig. 2b). The cLeaf estimates derived from WMA accurately captured the spatial pattern in most areas with a similar magnitude (Fig. 2c), except for in needleleaf forests with an underestimation of around 0.20–0.30 kg m^{-2}. The MMEM failed to accurately represent the high cLeaf not only in broadleaf forests within tropical regions and needleleaf forests in northern ecosystems but also in savannas (Fig. S6). This discrepancy might be attributed to the fact that only two out of seven ecosystem models (CLM5.0 and CABLE-POP) captured the spatial pattern of annual mean cLeaf (Fig. S6). Fig. 2d illustrates the spatial distribution of the cLeaf trend derived from the

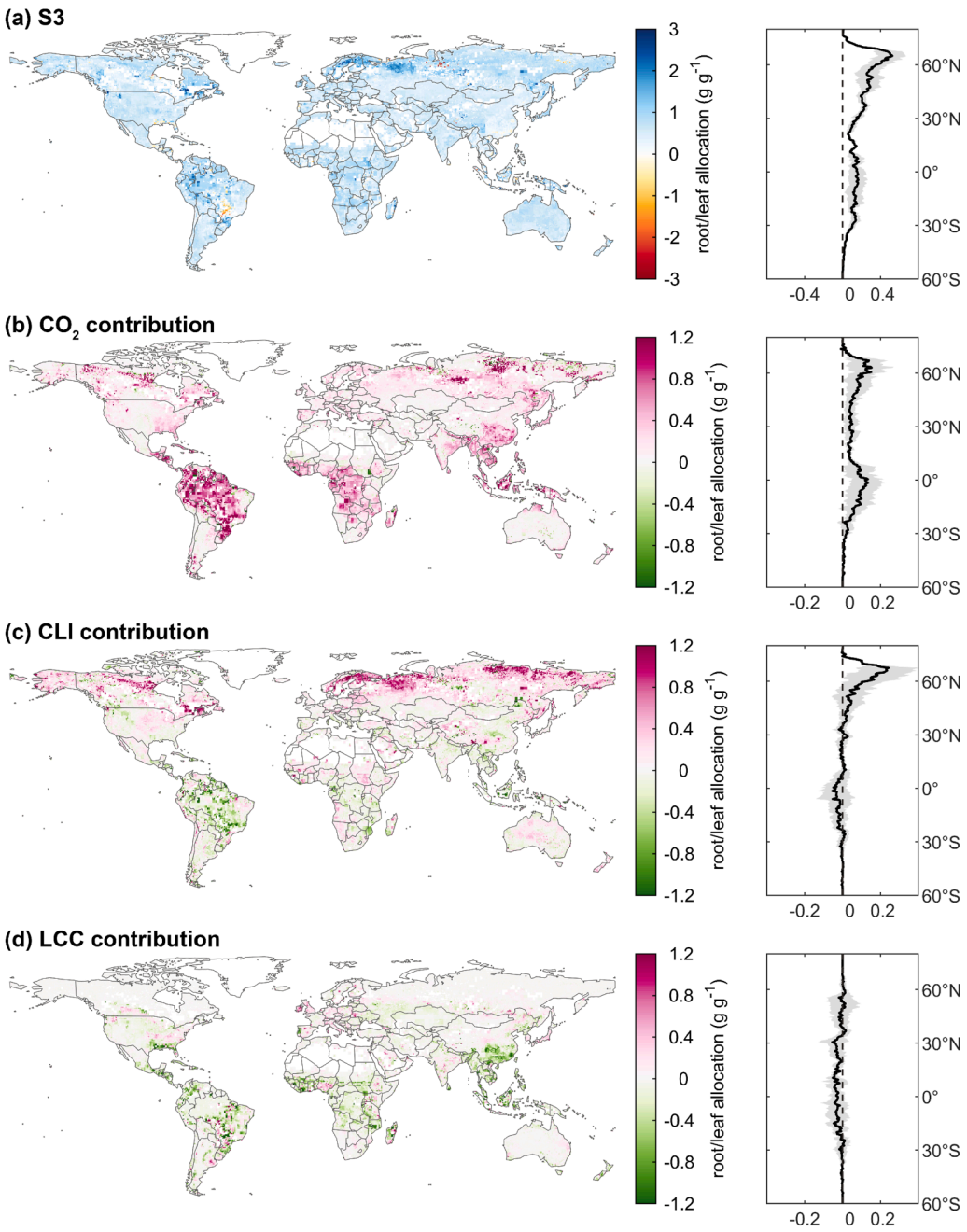

Fig. 5. Spatial patterns and drivers of global root/leaf carbon allocation between 1982 and 2018 from weighted model average (WMA). (*a*–*d*) show spatial patterns of (a) root/leaf carbon allocation (S3), (b) the effects of CO_2 concentrations, (c) the effects of climate change (CLI), and (d) the effects of changes in land use and land cover (LCC). The spatial patterns aggregated by latitude are in the left panel (black line), and the gray shades show the standard deviation.

observation data. A majority of regions exhibited an increasing cLeaf over the past 35 years, with exceptions in scattered areas within the middle and southern regions of Canada and the northern area of Mongolia. Notably, cLeaf trends exceeding 0.80×10^{-3} kg m^{-2} yr^{-1} were evident in the central regions of China, India, western Eurasia, the southeastern portion of central South America, and the eastern sector of North America. WMA effectively captured trends in cLeaf (Fig. 2e), although with certain levels of underestimation persisted within India and the middle of China, where none of the ecosystem models captured the increasing trends in cLeaf (Fig. S7).

Estimates of WMA root carbon (cRoot) were consistent with the global cRoot dataset along the climate gradients (Fig. 3a-b), with a higher correlation relationship ($R^2 = 0.82$) (Fig. 3c) than that of MMEM (Fig. S8), though discrepancy existed among individual models (Fig. S9). Specifically, cRoot was highest in warm (e.g., temperature > 20 °C) and humid (precipitation > 4000 mm month^{-1}) regions. As precipitation decreased in colder regions (e.g., temperature < 25 °C), root carbon declined. WMA captured the high root carbon in warm and humid areas, a phenomenon shared by most ecosystem models (Fig. S9), but overestimated root carbon for tropical regions (temperature = 17–27 °C) (Fig. 3d). In addition, WMA underestimated root carbon in arid regions (precipitation < 500 mm month^{-1}) and regions where mean temperatures < 0 °C. Overall, model-based estimates of root carbon provided valid representations of reality under different forcing scenarios.

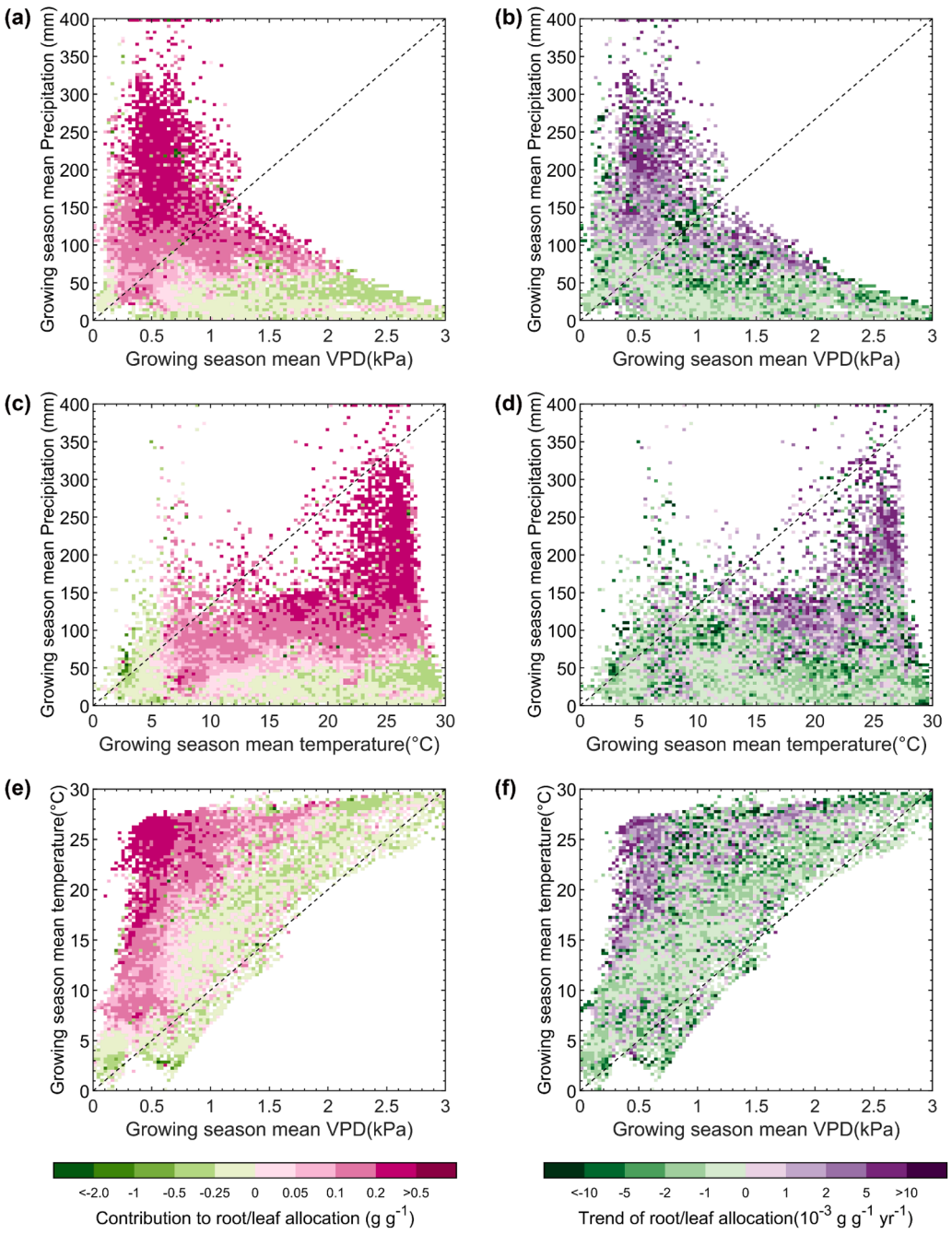

Fig. 6. Effects of CO_2 concentrations on root/leaf carbon allocation along the climate space based on the weighted model average (WMA). (a–c) show contributions of elevated CO_2 on root/leaf carbon allocation between 1982 and 2018. (d–f) show contributions of elevated CO_2 on the trend of root/leaf carbon allocation. The effects of CO_2 concentrations on root/leaf carbon allocation were plotted against binned values at mean growing season temperature of 0.3 °C intervals, mean growing season precipitation of 4-mm intervals and mean growing season VPD of 0.03 kPa intervals using climate conditions from 1901 to 1920.

3.3. Changes in global vegetation root/leaf carbon allocation and its drivers

We estimated root/leaf carbon allocation of global vegetation using WMA. The root/leaf carbon allocation was 0.582 ± 0.140 g g^{-1} ($p <$ 0.05) (Fig. 4a), and there was a significant trend of preferential carbon allocation to roots between 1982 and 2018 (0.0014 ± 0.0013 g g^{-1} yr^{-1}, $p < 0.05$) (Fig. 4b, 4c). WMA suggested that the increased allocation to roots was mainly due to increased CO_2 (0.218 ± 0.087 g g^{-1}) and that the effects of CO_2 have been continuous since 1982 (0.0010 ± 0.0005 g g^{-1} yr^{-1}, $p < 0.05$) (Fig. 4d). The contribution of climate change on root/leaf carbon allocation was insignificant (0.031 ± 0.055 g g^{-1}), as well as on the temporal changes (0.0002 ± 0.0009 g g^{-1} yr^{-1}, $p = 0.50$) (Fig. 4e). We also found a significant negative effect of land use and land cover change on the trend in global root/leaf carbon allocation (–0.0003 ± 0.0006 g g^{-1} yr^{-1}, $p < 0.05$) (Fig. 4f).

The spatial and latitudinal patterns in global root/leaf carbon allocation and the driving factors are shown in Fig. 5 (Fig. S11). The largest root/leaf carbon allocation was primarily observed in the northern high latitudes, followed by the tropics, including the rainforests of South America, Southeast Asia and the Congo basin (Fig. 5a), with similar latitudinal characteristics in the trend of root/leaf carbon allocation (Fig. S12, S13a). Over 54.6 % of global vegetation had an increased root/leaf carbon allocation trend except for regions in the middle of

Australia, the East African plateau, Central South America, and southwest China.

The root/leaf carbon allocation was dominated by different factors on the global scale. WMA indicated that more carbon was allocated to roots under a scenario of increasing atmospheric CO_2 concentrations throughout 82.4 % of the world, particularly in tropical regions (Fig. 5b). The effects of CO_2 were most evident in equatorial regions, including eastern India, Southeast Asia, and southeast China, and pronounced in certain parts of the northern hemisphere, including Canada, eastern America, and central Eurasia. Along latitudinal gradients, the CO_2 contribution on root/leaf carbon allocation trend was only remarkable around 10°N–10°S (Fig. S13b). Partial areas of decreased trend in leaf carbon were observed in eastern Africa, eastern South America, central North America, and northern Australia. Compared with the uniform spatial patterns of the effects of CO_2, the effects of climate change varied by latitude (Fig. 5c). Climate change led to increased carbon allocation to roots in the northern high latitudes, whereas more carbon was allocated to leaves in tropical rainforest regions and Southeast Asia. Similar patterns were shown in its contribution to the trend of root/leaf carbon allocation (Fig. S13c). The effects of changes in land use and land cover were less pronounced than those of CO_2 and climate change. Changes in land use and land cover led to increased carbon allocation to leaves throughout most of the world, but not in central South America, eastern America, Western Europe, Japan, Indonesia, or Eastern Australia (Fig. 5d, S13d).

3.4. Effects of CO_2 on root/leaf carbon allocation

Vegetation allocated more carbon to their roots as atmospheric CO_2 concentrations increased compared with the other two effects. To further investigate the underlying mechanisms, we examined the effects of CO_2 concentrations according to the climate space in the growing season (Fig. 6, Fig. S14–S15). As precipitation during the growing season increased, more carbon was allocated to the roots under elevated CO_2 concentrations, particularly when precipitation > 100 mm month^{-1} and VPD was below approximately 2 kPa (Fig. 6a); meanwhile, carbon tended to be allocated to the leaves under relatively arid conditions (Fig. 6b). As the mean growing season temperature increased above 5 °C between 1982 and 2018, more carbon was allocated to the roots (Fig. 6c). Such a trend in root allocation was consistent only when the temperature exceeds 15 °C (Fig. 6d). In warm and arid regions, plants allocated more carbon to leaves, whereas carbon was preferentially allocated to roots in relatively warm and humid areas (Fig. 6e, f).

4. Discussion

4.1. Mechanisms driving CO_2-induced changes in leaf-root carbon allocation

Observationally constrained TRENDY model outputs indicated that elevated CO_2 concentrations accounted for the increased root/leaf carbon allocation over the past 37 years. Recent studies have supported this phenomenon not only at the site scale but also at the global scale. For example, root carbon increased more than leaf carbon in mature forests under CO_2 enrichment at the ecosystem level (Jiang et al., 2020). Another evidence in the Duke FACE study related to broadleaved forests supported more carbon was allocated to roots than that of aboveground, particularly when light was a limiting factor (Maier et al., 2022). Global meta-analyses have found that rising CO_2 leads to increased root-to-shoot ratios, and that root length might be the main driver of these increases (Nie et al., 2013; Song et al., 2019). The process-based models also predicted that root allocation increased with elevated CO_2 concentrations under conditions of nutrient limitation (DeKauwe et al., 2014). Therefore, we suggested that nutrient limitation may mediate the effect of elevated CO_2 on the preferential allocation of carbon to roots.

First, nitrogen and phosphorus limitation occurred in northern ecosystems and tropical regions, respectively (Du et al., 2020), consistent with the patterns of large root/leaf carbon allocation in this study (Fig. 5b, Fig. 6). Considering that nutrients constrained the CO_2 effect on plant biomass (Cunha et al., 2022; Maier et al., 2022; Terrer et al., 2019), and nitrogen and phosphorus addition can promote aboveground biomass allocation (Yan et al., 2019b), we infer that more carbon is allocated to the root than to leaves to facilitate belowground nutrient uptake and sustain the vegetation growth under elevated CO_2. However, the models that we used, except for ORCHIDEE-CNP, neglect the phosphorus cycle. Additional components of the nutrient cycle should be incorporated into ecosystem models.

Second, soil water is another mediator of CO_2 contribution to root carbon allocation. A previous study suggested that more carbon was allocated to roots under rising CO_2 concentrations when soil water was limited (Wang and Taub, 2010). Another study found that the effects of CO_2 concentrations on pine were non-significant when soil resources were adequate (Maier et al., 2022). This means that the limitation of soil water leads to more carbon allocated to roots under elevated CO_2, and if the limitation was relieved, the carbon might be allocated to leaves. Our research found that carbon tended to be allocated to leaves in hyper-arid regions under elevated CO_2 concentrations (Fig. 6a, b). This phenomenon matches our expectations, as both rising CO_2 concentrations and aridity can promote stomatal closure (Wullschleger et al., 2002), which in turn improves water use efficiency and reduces water stress on roots (Gonsamo et al., 2021). In this situation, more carbon will be allocated to leaves.

Third, ecosystem type is another factor of carbon allocation in elevated CO_2. Ecosystems with mycorrhizal type that provides high nitrogen availability, such as boreal and temperate forests, respond more strongly in total and belowground biomass under elevated CO_2 (Terrer et al., 2016). In our results, temperate forests in northern high latitudes displayed the pattern of more root carbon allocation in response to elevated CO_2 concentration. However, the mycorrhizal type has seldom been mentioned in previous studies about carbon allocation (Song et al., 2019). Thus, to accurately estimate root/leaf carbon allocation, models need to incorporate factors such as nitrogen and phosphorus cycles.

4.2. Climate change effects on root/leaf carbon allocation

The contribution of climate change on carbon allocation varied with latitudes. Our results from WMA displayed that in the northern high latitudes climate change increased carbon allocation to roots, and this effect gradually disappeared with decreasing latitude (Fig. 5, S13c). Before attributing the potential contribution of climate change, we isolated the contribution of shifts in plant functional types (PFT) influenced by climate change (Diaz and Cabido, 1997). We found that the PFT schemes of global vegetation remained relatively stable in ecosystem models under climate change (Fig. S16). Therefore, the indirect contribution on carbon allocation induced by the PFT shifts in ecosystem models can be almost neglected compared with the direct contribution of elevated CO_2 and climate change. In tropical regions, carbon was preferentially allocated to leaves under a climate change scenario. Temperature is one of the main reasons for root/leaf carbon allocation patterns in northern high latitudes. In forest ecosystems, the temperature can predict biomass allocation patterns. Under increasingly cold climates, root carbon pools are larger than foliage pools (Reich et al., 2014a) due to low nutrient cycling rates (Gill and Jackson, 2000), which are constrained by temperature due to environmental adaptation. In addition, in warming conditions, vegetation displayed prolonged belowground growing season length (Liu et al., 2022), and woody plants have the advantage of resisting water stress with deeper root distributions and higher water use efficiency, thereby providing more time for the allocation of carbon to roots and in turn providing more water and nutrients to sustain larger growth despite warming (Song et al., 2019).

Change in water availability under climate change is also a vital factor in root/leaf carbon allocation. Previous studies have reported a

significant increase in the root biomass fraction and a decrease in the leaf biomass fraction under soil water stress (Eziz et al., 2017; Poorter and Nagel, 2000). In this study, we illustrated that more carbon was allocated to leaves than roots in tropical regions (Fig. 5c), where precipitation is abundant. The increases in mean annual precipitation can lead to decreased carbon allocation to roots (Roa-Fuentes et al., 2012), and increased allocation to wood and leaves (Yang et al., 2021). However, some studies found that carbon allocation among different organs appeared to be stable under drought stress (Cheng et al., 2009; Eziz et al., 2017), which might be related to their biomass allocation index being different from that in this study.

Light also accounts for the climate change effects on carbon allocation. Increased carbon allocation to leaves is expected under conditions of light limitation, such as in tropical regions where clouds associated with abundant precipitation reduce light availability for vegetation. In these regions, more carbon is expected to be allocated to leaves for photosynthesis (Graham et al., 2003) and to stems to increase height for light competition (Yang et al., 2021). Previous research has reported that shade, which may be caused by clouds or atmospheric particles, can notably impact vegetation productivity (Roderick et al., 2001). Additionally, the canopy itself creates shade, directly influencing gross primary productivity in the understory (Butler et al., 2020). Under such light-limited conditions, particularly within dense canopies with overlapping leaves, plants typically allocate more carbon to leaf production to enhance light capture. These light-driven shifts in carbon allocation are frequently intertwined with the effects of precipitation, which can also influence the allocation of carbon between leaves and roots. However, state-of-the-art ecosystem models generally do not represent these allocation processes accurately, due to both limited availability of detailed global light environment data and incomplete understanding of the underlying mechanisms.

4.3. Contribution of land cover and land use change to root/leaf carbon allocation

In this study, land cover and land use changes were associated with increased leaf carbon (decreased root/leaf carbon allocation) in most regions (Fig. 5d, S13d); however, in some places (e.g., western Europe), such changes contributed to increased root/leaf carbon allocation and its trend. One of the primary reasons for changes in carbon allocation patterns is the variation in vegetation types, driven by the inherent differences in plant traits across diverse vegetation types. For example, root-to-shoot ratios are highest in the tundra, grasslands, and cold deserts, and relatively low in forests and croplands (Jackson et al., 1996); thus, land cover changes involving conversion to a different vegetation type may lead to changes in allocation. Increases in the proportion of vegetation with low root-shoot ratios or decreases in the proportion of vegetation with high root-shoot ratios will likely lead to increases in leaf carbon and vice versa. Increases in croplands and forests in southeastern China, India, and Southeast Asia (Chen et al., 2019; Liu et al., 2020; Zhu et al., 2016) resulted in a relatively high proportion of leaf carbon during land cover changes. A trend toward increased root carbon has been observed in western Europe, central Africa, and eastern Australia, mirroring geographic patterns of cropland losses and grassland gains (Liu et al., 2020). These land cover changes converted low root-to-shoot ratio vegetation to a type with a higher ratio. Therefore, the inclusion of land cover and land use changes in models can lead to more accurate predictions. Human management may also alter allocation patterns; for example, farming promotes carbon allocation to leaves (Fraterrigo et al., 2006), and grazed grasslands in Tibet exhibited higher allocation to roots compared to exclosures (Hong et al., 2016). However, current models cannot accurately simulate the changes in land cover for complex human-managed systems, further influencing the contribution of land cover change on carbon allocation, and this problem is expected to be addressed in the future (Fisher et al., 2014).

4.4. N deposition contributes little to root/leaf carbon allocation

Although nitrogen is known to influence carbon allocation (Shipley and Meziane, 2002), only three ecosystem models (CLM5.0, ORCHIDEE-CNP, and LPX-Bern) incorporated nitrogen-related processes in our study. CLM5.0 and ORCHIDEE-CNP showed that nitrogen deposition promoted carbon allocation to leaves (–0.0009 g g^{-1} and –0.0466 g g^{-1}, respectively), whereas LPX-Bern predicted increased allocation to roots (0.0022 g g^{-1}). The result of ORCHIDEE-CNP may be attributable to its higher nitrogen sensitivity for leaves (Yan et al., 2019a). We thus compared the probability density functions of two simulations, one that integrated nitrogen deposition and one that did not, for each of the above three models (Fig. S17a-c). Our analysis presented that only ORCHIDEE-CNP displayed a significant contribution of nitrogen deposition on carbon allocation. The results were consistent with a recent global-scale meta-analysis (Yue et al., 2021) that nitrogen had little impacts on root and leaf carbon allocation at the global scale. The carbon allocation formulas of the three models differed (Table 1): CLM5.0, ORCHIDEE-CNP, and LPX-Bern use allometric, optimal, and allometric-optimal carbon allocation strategies, respectively. Thus, at the global scale, we can infer that the effects of nitrogen deposition follow the allometric relationship between roots and leaves, and might be influenced little by nitrogen deposition. We further analyzed the effects of nitrogen deposition on spatial patterns (Fig. S17d-f) and found that the responses to nitrogen deposition were consistent with their allocation strategies at the pixel scale. Models based on optimal theory (LPX-Bern and ORCHIDEE-CNP) predicted higher carbon allocation in magnitude.

4.5. Uncertainties and future directions

There were uncertainties from both observations and ecosystem models in our attempt to understand the changes in root/leaf carbon allocation. As for the observations, the first uncertainty source is the global carbon density references. The observational datasets of SLA and RMF were extrapolated through the Bayesian spatial model and machine learning model. These observational dataset from advanced extrapolation method can better explain the spatial variation compared with empirical upscaling. Particularly, the global RMF dataset was generated by over 63 information layers and illustrated an overestimation of root carbon in ecosystem models, therefore it provides a wealth of information on spatial variation in root carbon and is worth further investigation. However, obvious uncertainties arise from the prediction uncertainty located in the middle Asia of needleleaf forests and North America of savannas from the RMF dataset, while the SLA values of needleleaf forests in Northern ecosystems show smaller uncertainties than those of grasslands and savannas. Besides, we supposed that the SLA and RMF are time-constant because of the limited data availability. Such a simplification fails to capture the interannual variation. For example, the SLA has temporal changes in response to precipitation as well as anthropogenic events (Asefa et al., 2021; Dwyer et al., 2014; Poorter and Bongers, 2006), and the interspecies-specific leaf area in tropical regions usually gives large diversity (Butler et al., 2017; Reich et al., 2014b). Similarly, the root carbon varies with local site characteristics though its change is insignificant (Akburak et al., 2013). The root/leaf carbon allocation in this study relies on both interannual variation of root carbon and leaf carbon, while we only relied largely on the observed temporal changes of leaf carbon that is from quite detailed long-term satellite LAI. We use the spatial pattern of leaf carbon and root carbon can assist if over/underestimation exists. Another uncertainty source is the inconsistency among long-term LAI products (Jiang et al., 2017). To overcome it, we used the average of three LAI products as the reference in this article. Previous research (Anav et al., 2013) regarded it as acceptable once the errors from reference are smaller than those from model outputs (Fig. S5). Therefore, higher temporal accuracy in satellite observed LAI can serve as a better reference for WMA.

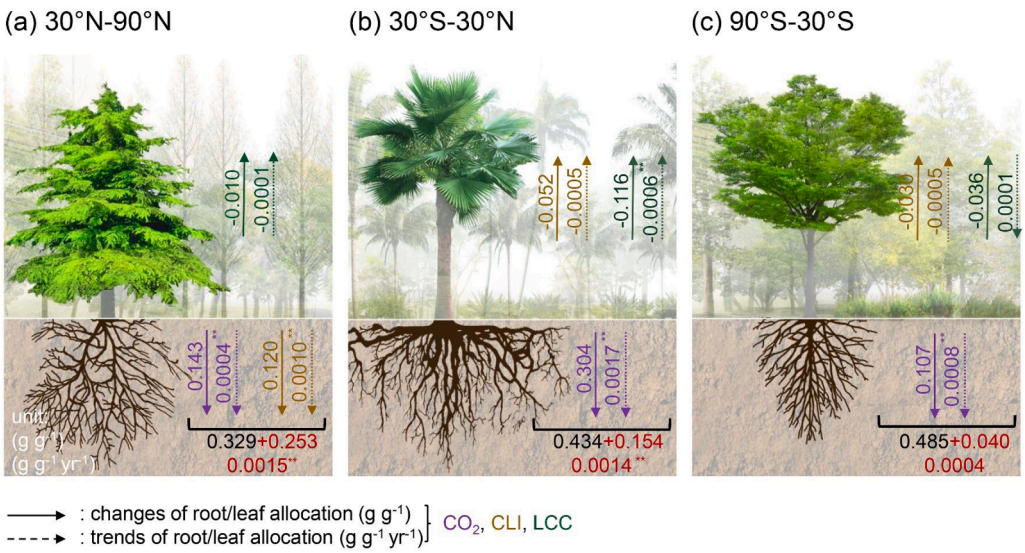

Fig. 7. Schematic presentation of global vegetation root/leaf carbon allocation pattern during 1982–2018. The regions are divided by latitudes, from left to right: 30°N∼90°N (a), 30°S∼30°N (b), and 90°S∼30°S (c) respectively. See legends for the corresponding arrows and units. The values in black are the root/leaf carbon allocation under S0, and the values in red indicate the contribution of global change (that is, the divergence between S3 and S0) to root/leaf carbon. The asterisks illustrate that the trend is statistically significant ($p < 0.05$).

In aspects of ecosystem models, we attribute the model uncertainty to the intrinsic processes and parameters. We noticed an underestimation of leaf carbon in needleleaf forests (Fig. 2c), and found it was related to the coarse description of leaf traits especially for needleleafforests in the state-of-art models (Reich et al., 2014b). Similarly, the vertical foliage profile was another important parameter for leaf carbon (Heimann and Reichstein, 2008; Tang et al., 2016). PFT is a significant determinant in woody carbon allocation (Puglielli et al., 2021), but the simplified PFT of global vegetation has been regarded as inadequate to describe carbon allocation (Butler et al., 2017). Therefore, adequate divisions with detailed vegetation trait values can promote the simulation of vegetation carbon accuracy (Ma et al., 2023), and the number of carbon pools is positively related to the accuracy of carbon allocation estimates in Earth system models (Song et al., 2017) because more allocation parameters can be represented for different PFT. Our results also suggest that models with more carbon pools, such as ORCHIDEE, CLM5.0, and ISAM, perform better. Noted that models employed fixed carbon allocation strategy (CLM5.0 and CABLE-POP) ranked the highest in the integrated performance of leaf carbon and root carbon, followed by four models using resources-limitation strategy, while the model optimal-allometric (LPX-Bern) performed worst. The phylogenetic effect is one of the most important contributors to allocation (Poorter et al., 2012). For example, belowground biomass in young trees increased more than aboveground biomass under conditions of elevated CO_2 (De Graaff et al., 2006). However, but phylogenetic effect fails to incorporate into ecosystem models at current stage. Overall, the incorporated vegetation allocation strategies varied among models, and the mechanism of carbon allocation is still far from being modeled (Fatichi et al., 2019).

5. Conclusions

Our observational constrained results from models have shown that more carbon was allocated to the root than to the leaf under global environmental changes since 1982 (Fig. 7). In northern high latitudes, climate change and increased atmospheric CO_2 concentration promoted more carbon allocated to the root than to leaves. Only subtle effects of land use and land cover change on leaf carbon allocation were found. Tropical regions were another hotspot in root/leaf carbon allocation with an enormous influence of the elevated atmospheric CO_2 concentration, which was partly counterbalanced by the contribution of land cover change and climate change. In southern high latitudes, land use and land cover change along with elevated CO_2 concentration were beneficial to leaf carbon allocation. Though the driving factors were divergent at the global scale, elevated CO_2 concentration was the main cause for more root carbon allocation in most areas. Our research is of critical importance to reveal the mechanisms of root/leaf carbon allocation in the context of global environmental changes.

Data and code availability

The datasets we employed in this article were available through the open database, with attached the website links in Data and methods. All computer codes for the analysis of the data are available from the corresponding author upon reasonable request.

CRediT authorship contribution statement

Zeyu Duanmu: Writing – original draft, Software, Resources, Methodology, Investigation, Formal analysis. **Zaichun Zhu:** Writing – review & editing, Writing – original draft, Supervision, Resources, Funding acquisition, Conceptualization. **Weiqing Zhao:** Writing – review & editing, Resources. **Anping Chen:** Writing – review & editing. **Zhaoqi Wang:** Writing – review & editing. **Sen Cao:** Writing – review & editing. **Dajing Li:** Writing – review & editing. **Yuhang Luo:** Resources. **Ranga B. Myneni:** Writing – review & editing.

Declaration of competing interest

The authors declare that they have no known competing financial interests or personal relationships that could have appeared to influence the work reported in this paper.

Acknowledgments

This research was supported by the National Natural Science Foundation of China (42271104, 42471103) and the Shenzhen Science and Technology Program (JCYJ20220531093201004). We thanked the TRENDY modelling group for providing the TRENDYv8 models data. We were grateful to the reviewers for their suggestions in this paper.

Supplementary materials

Supplementary material associated with this article can be found, in the online version, at doi:10.1016/j.agrformet.2024.110366.

Data availability

Data will be made available on request.

References

Aarssen, L.W., Taylor, D.R., 1992. Fecundity allocation in herbaceous plants. Oikos. 65 (2), 225–232.
Akburak, S., et al., 2013. Temporal variations of biomass, carbon and nitrogen of roots under different tree species. Scand. J For. Res. 28 (1), 8–16.
Anav, A., et al., 2013. Evaluating the land and ocean components of the global carbon cycle in the CMIP5 earth system models. J. Clim. 26 (18), 6801–6843.
Arora, V.K., Boer, G.J., 2005. A parameterization of leaf phenology for the terrestrial ecosystem component of climate models. Glob. Chang. Biol. 11 (1), 39–59.
Asaadi, A., et al., 2018. An improved parameterization of leaf area index (LAI) seasonality in the Canadian land surface scheme (CLASS) and Canadian terrestrial ecosystem model (CTEM) modelling framework. Biogeosciences 15 (22), 6885–6907.
Asefa, M., et al., 2021. Temporal trait plasticity predicts the growth of tropical trees. J. Vegetat. Sci. 32 (4), e13056.
Bloom, A.A., et al., 2016. The decadal state of the terrestrial carbon cycle: global retrievals of terrestrial carbon allocation, pools, and residence times. Proc. Natl. Acad. Sci. 113 (5), 1285–1290.
Bloom, A.J., et al., 1985. Resource limitation in plants-an economic analogy. Annu. Rev. Ecol. Syst. 16 (1), 363–392.
Borden, K.A., et al., 2021. Root functional trait and soil microbial coordination: implications for soil respiration in riparian agroecosystems. Front. Plant Sci. 12.
Buffam, I., et al., 2011. Integrating aquatic and terrestrial components to construct a complete carbon budget for a north temperate lake district. Glob. Chang. Biol. 17 (2), 1193–1211.
Butler, E.E., et al., 2020. Seeing the canopy for the branches: improved within canopy scaling of leaf nitrogen. J. Adv. Model. Earth. Syst. 12 (10).
Butler, E.E., et al., 2017. Mapping local and global variability in plant trait distributions. Proc. Natl. Acad. Sci. 114 (51), E10937–E10946.
Chen, C., et al., 2019. China and India lead in greening of the world through land-use management. Nat. Sustain. 2 (2), 122–129.
Cheng, D., et al., 2009. Invariant allometric relationship between above- and below-ground biomass along a moisture gradient in North - West China. Pol. J. Ecol. 57, 669–675.
Cunha, H.F.V., et al., 2022. Direct evidence for phosphorus limitation on Amazon forest productivity. Nature 608 (7923), 558–562.
De Graaff, M.-A., et al., 2006. Interactions between plant growth and soil nutrient cycling under elevated CO2: a meta-analysis. Glob. Chang. Biol. 12 (11), 2077–2091.
DeKauwe, M.G., et al., 2014. Where does the carbon go? A model-data intercomparison of vegetation carbon allocation and turnover processes at two temperate forest free-air CO2 enrichment sites. N. Phytol. 203.
Diaz, S., Cabido, M., 1997. Plant functional types and ecosystem function in relation to global change. J. Vegeta. Sci. 8 (4), 463–474.
Dijkstra, F.A., et al., 2021. Root effects on soil organic carbon: a double-edged sword. N. Phytol. 230 (1), 60–65.
Dolezal, J., et al., 2021. Contrasting biomass allocation responses across ontogeny and stress gradients reveal plant adaptations to drought and cold. Funct. Ecol. 35 (1), 32–42.
Du, E., et al., 2020. Global patterns of terrestrial nitrogen and phosphorus limitation. Nat. Geosci. 13 (3), 221–226.
Dwyer, J.M., et al., 2014. Specific leaf area responses to environmental gradients through space and time. Ecology 95 (2), 399–410.
El-Masri, B., et al., 2013. Carbon dynamics in the Amazonian Basin: integration of eddy covariance and ecophysiological data with a land surface model. Agric. For. Meteorol. 182-183, 156–167.
Enquist, B.J., Niklas, K.J., 2002. Global allocation rules for patterns of biomass partitioning in seed plants. Science (1979) 295 (5559), 1517–1520.
Exbrayat, J.F., et al., 2018. Reliability ensemble averaging of 21st century projections of terrestrial net primary productivity reduces global and regional uncertainties. Earth Syst. Dynam. 9 (1), 153–165.
Eyring, V., et al., 2019. Taking climate model evaluation to the next level. Nat. Clim. Chang. 9 (2), 102–110.
Eziz, A., et al., 2017. Drought effect on plant biomass allocation: a meta-analysis. Ecol. Evol. 7 (24), 11002–11010.
Fatichi, S., et al., 2019. Modelling carbon sources and sinks in terrestrial vegetation. N. Phytol. 221 (2), 652–668.
Fisher, J.B., et al., 2014. Modeling the terrestrial biosphere. Annu. Rev. Environ. Resour. 39 (1), 91–123.
Flato, G., et al., 2013. Evaluation of Climate Models. Cambridge University Press, Cambridge.
Franklin, O., et al., 2012. Modeling carbon allocation in trees: a search for principles. Tree Physiol. 32 (6), 648–666.
Fraterrigo, J.M., et al., 2006. Previous land use alters plant allocation and growth in forest herbs. J. Ecol. 94 (3), 548–557.
Friedlingstein, P., et al., 1999. Toward an allocation scheme for global terrestrial carbon models. Glob. Chang. Biol. 5 (7), 755–770.
Friend, A.D., et al., 2014. Carbon residence time dominates uncertainty in terrestrial vegetation responses to future climate and atmospheric CO2. Proc. Natl. Acad. Sci. 111 (9), 3280–3285.
Gill, R.A., Jackson, R.B., 2000. Global patterns of root turnover for terrestrial ecosystems. N. Phytol. 147 (1), 13–31.
Giorgi, F., Mearns, L., 2002. Calculation of average, uncertainty range, and reliability of regional climate changes from AOGCM simulations via the reliability ensemble averaging (REA) method. J. Clim. 15, 1141–1158.
Gonsamo, A., et al., 2021. Greening drylands despite warming consistent with carbon dioxide fertilization effect. Glob. Chang. Biol. 27 (14), 3336–3349.
Graham, E.A., et al., 2003. Cloud cover limits net CO2 uptake and growth of a rainforest tree during tropical rainy seasons. Proc. Natl. Acad. Sci. 100 (2), 572–576.
Hagedorn, F., et al., 2016. Recovery of trees from drought depends on belowground sink control. Nat. Plants. 2 (8), 16111.
Harris, I., et al., 2020. Version 4 of the CRU TS monthly high-resolution gridded multivariate climate dataset. Sci. Data 7 (1), 109.
Heimann, M., Reichstein, M., 2008. Terrestrial ecosystem carbon dynamics and climate feedbacks. Nature 451 (7176), 289–292.
Hong, J., et al., 2016. Leaf meristems: an easily ignored component of the response to human disturbance in alpine grasslands. Ecol. Evol. 6 (8), 2325–2332.
IPCC, 2021. Climate Change 2021: the Physical Science Basis. Working Group I Contribution to the IPCC Sixth Assessment Report, Cambridge, United Kingdom and New York, NY, USA.
Jackson, R.B., et al., 1996. A global analysis of root distributions for terrestrial biomes. Oecologia 108 (3), 389–411.
Jiang, C., et al., 2017. Inconsistencies of interannual variability and trends in long-term satellite leaf area index products. Glob. Chang. Biol. 23 (10), 4133–4146.
Jiang, M., et al., 2020. The fate of carbon in a mature forest under carbon dioxide enrichment. Nature 580 (7802), 227–231.
Kala, J., et al., 2014. Influence of leaf area index prescriptions on simulations of heat, moisture, and carbon fluxes. J. Hydrometeorol. 15 (1), 489–503.
Knutti, R., 2010. The end of model democracy? Clim. Change 102 (3), 395–404.
Knutti, R., et al., 2017. A climate model projection weighting scheme accounting for performance and interdependence. Geophys. Res. Lett. 44 (4), 1909–1918.
Krinner, G., et al., 2005. A dynamic global vegetation model for studies of the coupled atmosphere-biosphere system. Global. Biogeochem. Cycles. 19 (1).
Lawrence, D.M., et al., 2019. The community land model version 5: description of new features, benchmarking, and impact of forcing uncertainty. J. Adv. Model. Earth Syst. 11 (12), 4245–4287.
Liu, H., et al., 2020. Annual dynamics of global land cover and its long-term changes from 1982 to 2015. Earth Syst. Sci. Data 12 (2), 1217–1243.
Liu, H., et al., 2018. Shifting plant species composition in response to climate change stabilizes grassland primary production. Proceedings Natl. Acad. Sci. 115 (16), 4051–4056.
Liu, H., et al., 2022. Phenological mismatches between above- and belowground plant responses to climate warming. Nat. Clim. Chang. 12 (1), 97–102.
Liu, Y., et al., 2012. Retrospective retrieval of long-term consistent global leaf area index (1981–2011) from combined AVHRR and MODIS data. J. Geophys. Res.: Biogeosci. 117 (G4).
Luo, Y., et al., 2003. Sustainability of terrestrial carbon sequestration: a case study in Duke Forest with inversion approach. Global. Biogeochem. Cycles. 17 (1).
Ma, H., et al., 2023. The global biogeography of tree leaf form and habit. Nat. Plants. 9 (11), 1795–1809.
Ma, H., et al., 2021. The global distribution and environmental drivers of aboveground versus belowground plant biomass. Nat. Ecol. Evol. 5 (8), 1110–1122.
Mahmud, K., et al., 2018. Inferring the effects of sink strength on plant carbon balance processes from experimental measurements. Biogeosciences 15 (13), 4003–4018.
Maier, C.A., et al., 2022. The response of coarse root biomass to long-term CO2 enrichment and nitrogen application in a maturing Pinus taeda stand with a large broadleaved component. Glob. Chang. Biol. 28 (4), 1458–1476.
McCarthy, M.C., Enquist, B.J., 2007. Consistency between an allometric approach and optimal partitioning theory in global patterns of plant biomass allocation. Funct. Ecol. 21 (4), 713–720.
Meng, F., et al., 2023. Climate change increases carbon allocation to leaves in early leaf green-up. Ecol. Lett. 26 (5), 816–826.
Mokany, K., et al., 2006. Critical analysis of root : shoot ratios in terrestrial biomes. Glob. Chang. Biol. 12 (1), 84–96.
Müller, I., et al., 2000. The effect of nutrient availability on biomass allocation patterns in 27 species of herbaceous plants. Perspect. Plant Ecol. Evol. Syst. 3 (2), 115–127.
Nie, M., et al., 2013. Altered root traits due to elevated CO2: a meta-analysis. Global Ecology and Biogeography 22 (10), 1095–1105.
Palmroth, S., et al., 2006. Aboveground sink strength in forests controls the allocation of carbon below ground and its [CO2]-induced enhancement. Proc. Natl. Acad. Sci. 103 (51), 19362–19367.
Pearcy, R.W., et al., 2005. Crown architecture in sun and shade environments: assessing function and trade-offs with a three-dimensional simulation model. N. Phytol. 166 (3), 791–800.
Poorter, H. and Nagel, O.W., 2000. The role of biomass allocation in the growth response of plants to different levels of light, CO2, nutrients and water: a quantitative review.
Poorter, H., et al., 2012. Biomass allocation to leaves, stems and roots: meta-analyses of interspecific variation and environmental control. N. Phytol. 193 (1), 30–50.

Poorter, L., Bongers, F., 2006. Leaf traits are good predictors of plant performance across 53 rain forest species. Ecology 87 (7), 1733–1743.
Puglielli, G., et al., 2021. Global patterns of biomass allocation in woody species with different tolerances of shade and drought: evidence for multiple strategies. N. Phytol. 229 (1), 308–322.
Reich, P.B., et al., 2014a. Temperature drives global patterns in forest biomass distribution in leaves, stems, and roots. Proc. Natl. Acad. Sci. U.S.A. 111 (38), 13721–13726.
Reich, P.B., et al., 2014b. Biogeographic variation in evergreen conifer needle longevity and impacts on boreal forest carbon cycle projections. Proc. Natl. Acad. Sci. 111 (38), 13703–13708.
Roa-Fuentes, L.L., et al., 2012. Plant biomass allocation across a precipitation gradient: an approach to seasonally dry tropical forest at Yucatán, Mexico. Ecosystems 15 (8), 1234–1244.
Roderick, M.L., et al., 2001. On the direct effect of clouds and atmospheric particles on the productivity and structure of vegetation. Oecologia 129 (1), 21–30.
Ruehr, S., et al., 2023. Evidence and attribution of the enhanced land carbon sink. Nat. Rev. Earth Environ. 4 (8), 518–534.
Ruesch, A.S. and Gibbs, H.K., 2008. New IPCC Tier-1 Global Biomass Carbon Map for the Year 2000.
Shipley, B., Meziane, D., 2002. The balanced-growth hypothesis and the allometry of leaf and root biomass allocation. Funct. Ecol. 16 (3), 326–331.
Sitch, S., et al., 2003. Evaluation of ecosystem dynamics, plant geography and terrestrial carbon cycling in the LPJ dynamic global vegetation model. Glob. Chang. Biol. 9 (2), 161–185.
Song, J., et al., 2019. A meta-analysis of 1,119 manipulative experiments on terrestrial carbon-cycling responses to global change. Nat. Ecol. Evol. 3 (9), 1309–1320.
Song, X., et al., 2017. Significant inconsistency of vegetation carbon density in CMIP5 Earth system models against observational data. J. Geophys. Res.: Biogeosci. 122 (9), 2282–2297.
Sun, Y., et al., 2021. Global evaluation of the nutrient-enabled version of the land surface model ORCHIDEE-CNP v1.2 (r5986). Geosci. Model Dev. 14 (4), 1987–2010.
Tang, H., et al., 2016. Characterizing leaf area index (LAI) and vertical foliage profile (VFP) over the United States. Biogeosciences. 13 (1), 239–252.
Terrer, C., et al., 2019. Nitrogen and phosphorus constrain the CO2 fertilization of global plant biomass. Nat. Clim. Chang. 9 (9), 684–689.
Terrer, C., et al., 2016. Mycorrhizal association as a primary control of the CO_2fertilization effect. Science (1979) 353 (6294), 72–74.
Thornley, J.H.M., 1972. A balanced quantitative model for root: shoot ratios in vegetative plants. Ann. Bot. 36 (145), 431–441.
Tian, D.-L., et al., 2010. Effects of thinning and litter fall removal on fine root production and soil organic carbon content in masson pine plantations. Pedosphere 20 (4), 486–493.
Vicca, S., et al., 2012. Fertile forests produce biomass more efficiently. Ecol. Lett. 15 (6), 520–526.
Wang, X., Taub, D.R., 2010. Interactive effects of elevated carbon dioxide and environmental stresses on root mass fraction in plants: a meta-analytical synthesis using pairwise techniques. Oecologia 163 (1), 1–11.
Wang, Y.p., et al., 2009. A global model of carbon, nitrogen and phosphorus cycles for the terrestrial biosphere. Biogeosciences 7, 2261–2282.
Wullschleger, S.D., et al., 2002. Plant water relations at elevated CO2 – implications for water-limited environments. Plant Cell Environ. 25, 319–331.
Xiao, Z., et al., 2014. Use of general regression neural networks for generating the glass leaf area index product from time-series MODIS surface reflectance. IEEE Transa. Geosci. Remote Sens. 52 (1), 209–223.
Yan, Z. et al., 2019a. Biomass Allocation in Response to Nitrogen and Phosphorus Availability: insight From Experimental Manipulations of Arabidopsis thaliana. 10.
Yan, Z., et al., 2019b. Biomass allocation in response to nitrogen and phosphorus availability: insight from experimental manipulations of arabidopsis thaliana. Front. Plant Sci. 10.
Yang, H., et al., 2021. Variations of carbon allocation and turnover time across tropical forests. Glob. Ecol. Biogeogr. 30 (6), 1271–1285.
Yue, K., et al., 2021. Nitrogen addition affects plant biomass allocation but not allometric relationships among different organs across the globe. J. Plant Ecol. 14 (3), 361–371.
Zhao, Q., et al., 2020. Future greening of the Earth may not be as large as previously predicted. Agric. For. Meteorol. 292-293, 108111.
Zhao, W., Zhu, Z., 2022. Exploring the best-matching plant traits and environmental factors for vegetation indices in estimates of global gross primary productivity. Remote Sens. (Basel) 14 (24), 6316.
Zhou, L., et al., 2020. Responses of biomass allocation to multi-factor global change: a global synthesis. Agric. Ecosyst. Environ. 304, 107115.
Zhu, Z., et al., 2013. Global data sets of vegetation leaf area index (LAI)3 g and fraction of photosynthetically active radiation (FPAR)3 g derived from global inventory modeling and mapping studies (GIMMS) Normalized Difference Vegetation Index (NDVI3g) for the Period 1981 to 2011. Remote Sens. (Basel) 5 (2), 927–948.
Zhu, Z., et al., 2017. Attribution of seasonal leaf area index trends in the northern latitudes with “optimally” integrated ecosystem models. Glob. Chang. Biol. 23 (11), 4798–4813.
Zhu, Z., et al., 2016. Greening of the Earth and its drivers. Nat. Clim. Chang. 6 (8), 791–795.